Journal of Medical Entomology, 58(6), 2021, 2453–2466
doi: 10.1093/jme/tjab107
Advance Access Publication Date: 21 July 2021
Research

ENTOMOLOGICAL SOCIETY OF AMERICA
SHARING INSECT SCIENCE GLOBALLY

OXFORD

Vector/Pathogen/Host Interaction, Transmission

A Comparative Spatial and Climate Analysis of Human Granulocytic Anaplasmosis and Human Babesiosis in New York State (2013–2018)

Collin O'Connor,[1,13] Melissa A. Prusinski,[1] Shiguo Jiang,[2] Alexis Russell,[1,9,*] Jennifer White,[1] Richard Falco,[3] John Kokas,[3,12,*] Vanessa Vinci,[3] Wayne Gall,[4,11,*] Keith Tober,[4,12,*] Jamie Haight,[5] JoAnne Oliver,[6] Lisa Meehan,[1,10,*] Lee Ann Sporn,[7] Dustin Brisson,[8] and P. Bryon Backenson[1]

[1]New York State Department of Health, Bureau of Communicable Disease Control, Albany, NY, USA,[2]State University of New York, University at Albany, Department of Geography and Planning, Albany, NY, USA,[3]New York State Department of Health, Bureau of Communicable Disease Control, Armonk, NY, USA,[4]New York State Deparment of Health, Bureau of Communicable Disease Control, Buffalo, NY, USA,[5]New York State Department of Health, Bureau of Communicable Disease Control, Falconer, NY, USA,[6]New York State Department of Health, Bureau of Communicable Disease Control, Syracuse, NY, USA,[7]Paul Smith's College, Department of Natural Science, Paul Smiths, NY, USA,[8]University of Pennsylvania, Department of Biology, Philadelphia, PA, USA,[9]Wadsworth Center, Division of Infectious Disease, Albany, NY, USA,[10]Wadsworth Center, Division of Environmental Health Sciences, Albany, NY, USA,[11]United States Department of Agriculture, Animal and Plant Health Inspection Service, Buffalo, NY, USA,[12]Retired, and [13]Corresponding author, e-mail: collin.oconnor@health.ny.gov

*Denotes current affiliation.

Subject Editor: Sarah Hamer

Received 8 February 2021; Editorial decision 21 May 2021

Abstract

Human granulocytic anaplasmosis (HGA) and human babesiosis are tick-borne diseases spread by the blacklegged tick (*Ixodes scapularis* Say, Acari: Ixodidae) and are the result of infection with *Anaplasma phagocytophilum* and *Babesia microti*, respectively. In New York State (NYS), incidence rates of these diseases increased concordantly until around 2013, when rates of HGA began to increase more rapidly than human babesiosis, and the spatial extent of the diseases diverged. Surveillance data of tick-borne pathogens (2007 to 2018) and reported human cases of HGA (n = 4,297) and human babesiosis (n = 2,986) (2013–2018) from the New York State Department of Health (NYSDOH) showed a positive association between the presence/temporal emergence of each pathogen and rates of disease in surrounding areas. Incidence rates of HGA were higher than human babesiosis among White and non-Hispanic/non-Latino individuals, as well as all age and sex groups. Human babesiosis exhibited higher rates among non-White individuals. Climate, weather, and landscape data were used to build a spatially weighted zero-inflated negative binomial (ZINB) model to examine and compare associations between the environment and rates of HGA and human babesiosis. HGA and human babesiosis ZINB models indicated similar associations with forest cover, forest land cover change, and winter minimum temperature; and differing associations with elevation, urban land cover change, and winter precipitation. These results indicate that tick-borne disease ecology varies between pathogens spread by *I. scapularis*.

Key words: anaplasmosis, babesiosis, zero-inflated negative binomial regression model, climate, landscape

Human granulocytic anaplasmosis (HGA) and human babesiosis are tick-borne diseases caused by the pathogens *Anaplasma phagocytophilum* and *Babesia microti*, respectively (Spielman et al. 1985, Chen et al. 1994, Dumler et al. 2001). HGA and human babesiosis exhibit similar non-specific flu-like symptoms including fatigue, fever, chills, and headache (White et al. 1998, Ramsey 2002).

Both diseases may result in death (Bakken et al. 1996, White et al. 1998), however, most patients recover with appropriate antibiotic and antiparasitic treatments, respectively (White et al. 1998, Ramsey 2002).

In New York State (NYS), rates of HGA and human babesiosis had been increasing steadily and at similar rates since the early 2000s (Daniels et al. 1998; Kogut et al. 2005; New York State Department of Health 2006a, 2006b, 2011; Dahlgren et al. 2011, 2015; Joseph et al. 2011, 2020). However, rates of HGA have rapidly increased in recent years, surpassing those of human babesiosis (Fig. 1) (New York State Department of Health 2019). The recent surge of HGA cases is of interest when examined in the context of human babesiosis, as both HGA and human babesiosis are spread by the same vector species, the blacklegged tick or deer tick (*Ixodes scapularis* Say, Acari: Ixodidae) (Dennis et al. 1998, Homer et al. 2000) and have the same primary reservoir in nature, the white-footed mouse (*Peromyscus leucopus* Rafinesque (Rodentia: Cricetidae)) (Stafford et al. 2014, Stephenson and Foley 2016).

A potential explanation for diverging disease rates, despite similarities in the transmission pathway, is each pathogen's unique relationship to the environment. Assessing how the environment affects tick-borne disease risk is an important research topic, as it has allowed researchers to spatially forecast the risk of Lyme disease in response to the projections of a changing climate (Brownstein, Holford et al. 2005; Ogden et al. 2006, 2008). Studies have examined the direct effects of environmental characteristics on tick behavior (Vail and Smith 1998, Berger, Ginsberg, Dugas, et al. 2014,Berger, Ginsberg, Gonzalez et al. 2014), which relates to disease risk from all tick-borne pathogens. Recent studies have shown that environmental conditions can affect the microbiome composition of *I. scapularis* (Thapa et al. 2019) and *Dermacentor andersoni* Stiles (Acari: Ixodidae) (the rocky mountain wood tick) (Gall et al. 2016), providing evidence that environmental conditions affect tick-borne pathogens differently. Further, *I. scapularis* infected with *A. phagocytophilum* express an antifreeze glycoprotein, called *iafgp*, which gives *I. scapularis* an increased resistance to colder temperatures (Neelakanta et al. 2010). Despite evidence for pathogen-specific interactions with the environment, large-scale spatial ecology studies have generally only examined the effect of the environment and landscape characteristics on the spatial density of *I. scapularis* and the prevalence of *Borrelia burgdorferi* (the causative agent of Lyme disease) in *I. scapularis* populations (Diuk-Wasser et al. 2010, 2012; Khatchikian et al. 2012; Piedmonte et al. 2018). The relationship between environmental conditions and the prevalence of *A. phagocytophilum* or *B. microti* and their respective human illnesses remains at large spatial scales largely unstudied.

Varying climate and elevation in NYS may help to elucidate the potential effect of the environment on increasing rates of HGA and human babesiosis. The highest incidence rates of HGA and human babesiosis are localized to different regions of NYS (New York State Department of Health 2019); the upper and mid-Hudson Valley regions have exhibited the highest rates of HGA (New York State Department of Health 2018), while higher rates of human babesiosis have occurred in the lower Hudson Valley and the coastal region of Long Island (Kogut et al. 2005, New York State Department of Health 2018, Joseph et al. 2020).

This study aims to use a large-scale spatially-weighted regression to comparatively examine the association between the environment of NYS and the rates of HGA and human babesiosis. Further, this study examines tick pathogen surveillance data from the New York State Department of Health (NYSDOH) spatiotemporally, to describe changing pathogen prevalence of *A. phagocytophilum* and *B. microti* among *I. scapularis* populations across NYS.

Methods

Human Granulocytic Anaplasmosis and Human Babesiosis Case Criteria

Cases of HGA and human babesiosis occurring between 2013 and 2018 in NYS (excluding NYC) from the NYSDOH Communicable Disease Electronic Surveillance System (CDESS) were analyzed using SAS v. 9.2 (SAS Institute, https://www.sas.com). Suspected or confirmed cases of HGA and human babesiosis are reportable to the NYSDOH under New York State Sanitary Code (10NYCRR 2.10), and are assigned a case status according to the prevailing CDC case definitions at the time of reporting (Council of State and Territorial Epidemiologists 2008, 2011). Only cases recorded in CDESS with a case status of either "confirmed" or "probable" were included in this study. According to the Council of State and Territorial Epidemiologist (CSTE) 2008 case definition, a confirmed case of HGA is a case that meets clinical evidence criteria and is laboratory confirmed, while a probable case is a clinically compatible case that has supportive laboratory results. Similarly for human babesiosis, a confirmed case must meet subjective or objective clinical evidence criteria and have confirmatory laboratory results, while a probable case has objective clinical evidence criteria and supportive laboratory results. A probable case designation may be achieved through epidemiologic linkage via blood donation. More detailed

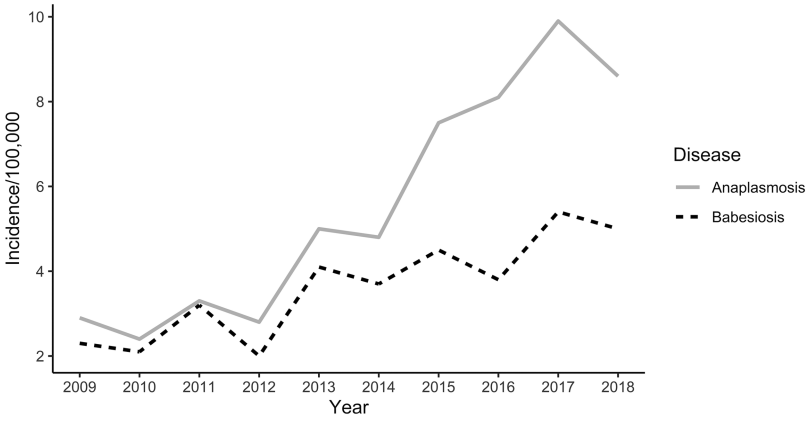

Fig. 1. Incidence of human granulocytic anaplasmosis and human babesiosis in New York State (2009–2018).

information regarding HGA and human babesiosis case designations is available from the CDC (https://wwwn.cdc.gov/nndss/conditions/ehrlichiosis-and-anaplasmosis/case-definition/2008/ https://wwwn.cdc.gov/nndss/conditions/babesiosis/case-definition/2011/). CDESS records contain multiple clinical and demographic fields used for disease surveillance, and variables included in this study were the United States Postal Service (USPS) ZIPcode of patient residence, clinical outcome, the year the case occurred, age, sex, race, and ethnicity. Clinical outcomes of cases are coded as either alive, dead or unknown, and are recorded to reflect the result of infection.

Case Demographics

Total population at risk and corresponding demographic distribution data were gathered from the American Community Survey (ACS) 2013 5-year estimates, aggregated to the spatial boundaries of ZIP code tabulation areas (ZCTAs) (United States Census Bureau 2013). ZCTAs are spatial geography used by the United States Census Bureau to spatially aggregate population count and demographic data gathered by the ACS and decennial census (United States Census Bureau 2000). Case data contain the specific ZIP code of each case's home address, which was manually converted to its corresponding ZCTA. Converting case data from ZIP code to ZCTA was required to spatially relate case counts of HGA and human babesiosis to the count and demographics of at-risk persons in the incidence rate calculation. Incidence rates of HGA and human babesiosis were then calculated for the 6-yr study period (2013–2018) and were weighted by age, sex, race, and ethnicity of each case and underlying population demographic distribution. Frequency distributions of HGA and human babesiosis cases were examined across age, sex, race, ethnicity, and clinical outcome variables via bar plots created in R v. 3.6.1 using the 'ggplot2' package (Wickham 2016, R Core Team 2019). Chi-square and Fisher's exact tests were performed to look for differences in the frequency of demographic categories between confirmed and probable cases. Bonferroni-Holm adjustment was used to correct for multiple comparisons ($\alpha = 0.05$) (Hochberg 1988). Stacked bar charts and choropleth maps were created using the 'ggplot2' and 'tmap' packages in R v. 3.6.1 (Tennekes 2018), and were used to visually examine for temporal and spatial variability in confirmed and probable cases of HGA and human babesiosis. Following examination of confirmed and probable cases, it was determined that combining confirmed and probable cases into a total case count was appropriate for further analysis.

Tick Sampling and Pathogen Testing

Host-seeking adult and nymphal tick sampling were conducted on publicly accessible lands from the period of 2007 to 2018 as described elsewhere (Prusinski et al. 2014). Adult *I. scapularis* were sampled via active tick flagging during the months of April and May for spring-questing adults and between October and December for fall-questing adults. Nymphal life-stage *I. scapularis* were sampled via active tick dragging between the months of May and September. During all initial site visits, GPS coordinates of the site were recorded to be used for spatial analysis, and environmental data such as ambient air temperature (°C) and relative humidity were recorded using a sling psychrometer. Estimated wind speed (mph), and general weather observations were also noted at the time of sampling. *I. scapularis* were identified under a dissecting microscope (Model SMZ1000, Nikon, Tokyo, Japan) to species utilizing dichotomous keys (Keirans and Clifford 1978, Keirans et al. 1996) and stored in 99.5% ethanol at –20°C until DNA extraction.

I. scapularis samples collected between 2007 and 2012 underwent total genomic DNA extraction via spin column method (DNeasy Blood and Tissue Kit, Qiagen USA, Germantown, MD), and were tested for the presence of (target gene): *A. phagocytophilum* (*msp3*), *B. microti* (*16S-like rRNA*), and *B. burgdorferi* (*ospA*) using a triplex Polymerase Chain Reaction (PCR) assay as described elsewhere (Prusinski et al. 2014). *I. scapularis* samples collected between 2013 and 2018 underwent automated total genomic DNA extraction via Qiagen QIAcube HT using QIAamp 96 kit (Qiagen USA, Germantown, MD) according to manufacturer protocols. Extracted DNA was then tested for the presence of (target gene) *A. phagocytophilum* (*msp2*), *B. microti* (*18S rDNA*), *B. burgdorferi* (*16S rDNA*), and *Borrelia miyamotoi* (*16S rDNA*) using a quadplex real-time PCR assay as previously described (Piedmonte et al. 2018).

Results for the presence of *A. phagocytophilum* and *B. microti* in *I. scapularis* ticks were linked to the corresponding collection site data. Collection sites were then characterized based on the first temporal occurrence for a PCR positive result for either *A. phagocytophilum* or *B. microti* separately among *I. scapularis*. Study sites were grouped as either: sites where no PCR positive results for a pathogen had been found, sites where one or more PCR positive results for a pathogen were found during or after 2013 (the human case study period), or sites where one or more PCR positive results for a pathogen were found before 2013 or on the first visit to a collection site after 2013.

Tick Pathogen Relation to Human Case Incidence

Incidence rates of HGA and human babesiosis during the period of 2013–2018 for each NYS ZCTA were merged to a TIGER/Line shapefile of NYS ZCTAs (United States Census Bureau 2019) in ArcMap v. 10.6.1 (ESRI 2018). Tick collection sites categorized according to the temporal emergence of *A. phagocytophilum* and *B. microti* in *I. scapularis* populations were mapped and intersected with the NYS ZCTA shapefile to determine which NYS ZCTAs contained each collection site. ZCTAs were then assigned the same category of temporal emergence of *A. phagocytophilum* and *B. microti* as collection sites located within them. In the event that a ZCTA contained more than one collection site, all observations from those collection sites were combined and reassessed as a single collection site, and the resulting category was assigned to the ZCTA. Incidence rates among the assigned categories of pathogen emergence were then analyzed using the non-parametric Kruskal–Wallis test ($\alpha = 0.05$) to determine whether the distribution of the incidence of HGA and human babesiosis differed between any of the three groups (Kruskal and Wallis 1952). Stepwise comparisons between temporal pathogen emergence groups were then assessed using the pairwise Wilcoxon rank-sum test (Dunn 1964) with Bonferroni-Holm correction ($\alpha = 0.05$) (Hochberg 1988) to determine whether temporal pathogen emergence groups had differing distributions of human incidence.

Climate/Weather and Landscape Data Collection

Climate, weather, and landscape variables were selected to represent variables significantly associated with tick density in the current literature. All climate and weather variables were gathered from Parameter-elevation Regressions on Independent Slopes Model (PRISM) (Tran and Waller 2013) as raster files (PRISM Climate Group, Accessed 2/2020). Variables gathered from PRISM included: precipitation (Burtis et al. 2016, Tran et al. 2020), mean temperature (Ashley and Meentemeyer 2004), minimum temperature, maximum temperature, mean dewpoint temperature (Berger, Ginsberg, Gonzalez, et al. 2014), minimum vapor

pressure deficit (Brownstein et al. 2003, Tran et al. 2020) and maximum vapor pressure deficit. Annual yearly averages and monthly averages for each PRISM variable were gathered and spatially averaged over each NYS ZCTA using the 'zonal statistics as table' tool in ArcMap during the study period (ESRI 2019). After a spatial average was calculated for each climate variable during its corresponding unit of time, values were averaged over the entire study to achieve single values for use in regression analysis. Winter averages were calculated as the average of each monthly value from November through March for each year from 2012 through 2018.

Landscape covariates were selected from significant tick density predictors in the published literature, including elevation (Arab 2015, Tran et al. 2020), deciduous and mixed forest cover (Guerra et al. 2002), and change in land use (Halos et al. 2010). Elevation data at 7.5 arc-second spatial resolution was gathered from the Global Multi-resolution Terrain Elevation Dataset (GMTED) 2010 in raster format (Danielson and Gesch 2011). 'Zonal statistics as table' was used to find the mean elevation for each NYS ZCTA. Land cover and land cover change data were gathered from the National Land Cover Database (NLCD) 2016 Land Cover and 2016 Land Cover Change Index (LCCI), respectively (Yang et al. 2018, Homer et al. 2020). The NLCD Land Cover dataset was used to assess the percent of a ZCTA's total area covered with deciduous or mixed forest. Deciduous and mixed forest layers were cut from the NYS ZCTA layer via the 'Erase' tool, leaving the total area for each ZCTA not covered with either deciduous or mixed forest. The remaining areas within each ZCTA were then used to calculate forest coverage percentages. This process was repeated to assess land cover change via the forest change and urban change layers in the NLCD LCCI. Both the forest and urban change layers indicate whether a spatial area has changed to or from its respective land cover class at any point between the period of 2001 and 2016.

Spatial Regression Model Development

Case counts of HGA and human babesiosis were predicted via environmental covariates using zero-inflated negative binomial (ZINB) regression model with ACS 2013 5-year population estimates as an offset. The goal of the model-building procedure was to assess the association of environmental factors with cases of HGA and human babesiosis. Traditionally, a Poisson regression model is used to assess count data (Mekonnen et al. 2019), but in the event of overdispersion, a negative binomial regression model is used (Chamberlain et al. 2017). Further, when the count data exhibits an excess of zero count observations in addition to overdispersion, the ZINB model may be used (Zhen et al. 2018). The ZINB model assumes that variation in the number of successes greater than zero and the process that determines if an observation is either zero or non-zero are independent (Bhowmik et al. 2020). To deal with the separate processes and excess zero counts, the ZINB model simultaneously assesses a negative binomial model for count values greater than zero, and a logistic model to measure the likelihood of being in the "not at risk" group (Preisser et al. 2012).

ZINB models for HGA and human babesiosis were built using a three-step process. First, a correlation matrix was created containing all environmental variables using the 'ggpairs' function from the 'GGally' package in R (Schloerke et al. 2018). Variables were then examined for high correlation using Pearson' correlation coefficient and iteratively removed from the correlation matrix. If the removal of a variable did not reduce the correlation between covariates, it was added back into the correlation matrix. This process was repeated until a sufficient amount of variables remained to answer the main research questions and kept all covariate correlation near 0.70. Second, all remaining variables were used to build a backwards-stepwise logistic regression model to determine which variables would be used to build the zero-inflated portion of the ZINB model (Diuk-Wasser et al. 2010). Finally, the ZINB model was built using the backwards stepwise method using the 'zeroinfl' function from the 'pscl' package in R (Zeileis et al. 2008). All variables were input into the negative binomial portion of the ZINB model and the significant variables from the previous logistic regression were input into the zero-inflated portion of the ZINB model. Variables were removed one by one when not statistically significant (α = 0.05), starting with the variable with the highest p-value.

After final models for HGA and human babesiosis were determined, their residuals were examined for spatial heterogeneity via Moran's I (Moran 1950), using inverse distance weighting of centroids of ZCTAs from the R 'spdep' package (α = 0.05) (Bivand and Wong 2018). If Moran's I revealed spatial heterogeneity in the model, a spatial autocovariate term was fitted to the final models to improve fit and control for the distance between sites (Dormann et al. 2007). Models with and without an autocovariate term were compared using AIC, where the best fit occurred if the spatially controlled model had an AIC value of two or more points less than the non-spatially controlled model.

Results

Human Granulocytic Anaplasmosis and Human Babesiosis Case Surveillance

A total of 4,297 cases of HGA (2,894 confirmed and 1,403 probable) and 2,986 cases of human babesiosis (2,440 confirmed and 546 probable) were reported between 2013 and 2018 in NYS (excluding NYC). Incidence of both HGA and human babesiosis increased over the study period, however, the increase of HGA incidence was of a higher magnitude and extended further northward than human babesiosis (Fig. 2). HGA and human babesiosis case demographics and final patient health outcomes are shown (Fig. 3, Table 1). Resulting health outcomes and demographics from a separate analysis of "confirmed" and "probable" case categories of HGA and human babesiosis are also summarized (Supp Tables S1 and S2 [online only]), with results of χ^2 and Fisher's exact tests examining potential differences in the demographic distribution by case classification of each disease detailed (Supp Table S3 [online only]). The frequency of confirmed and probable HGA and human babesiosis cases in NYS over time is also shown (Supp Fig. 1 [online only]). Total confirmed and probable cases in NYS aggregated to the ZCTA spatial scale are displayed as a choropleth map (Supp Fig. 2 [online only]).

Ixodes scapularis Testing Results and Temporal Pathogen Emergence

During the period of 2007 through 2018, 34,076 adult and 18,539 nymphal *I. scapularis* ticks were tested for *A. phagocytophilum* and *B. microti*. Among adult *I. scapularis* tested, 2,190 samples (6.43%) were positive for *A. phagocytophilum* and 1,209 samples (3.55%) were positive for *B. microti*. Among nymphal *I. scapularis* tested, 799 samples (4.31%) were positive for *A. phagocytophilum* and 674 samples (3.64%) were positive for *B. microti*. Additionally, 181 (0.53%) and 28 (0.15%) samples were simultaneously infected with both *A. phagocytophilum* and *B. microti* among adults and nymphs respectively.

PCR results for *A. phagocytophilum* and *B. microti* aggregated to 319 field collection sites to show temporal emergence of each

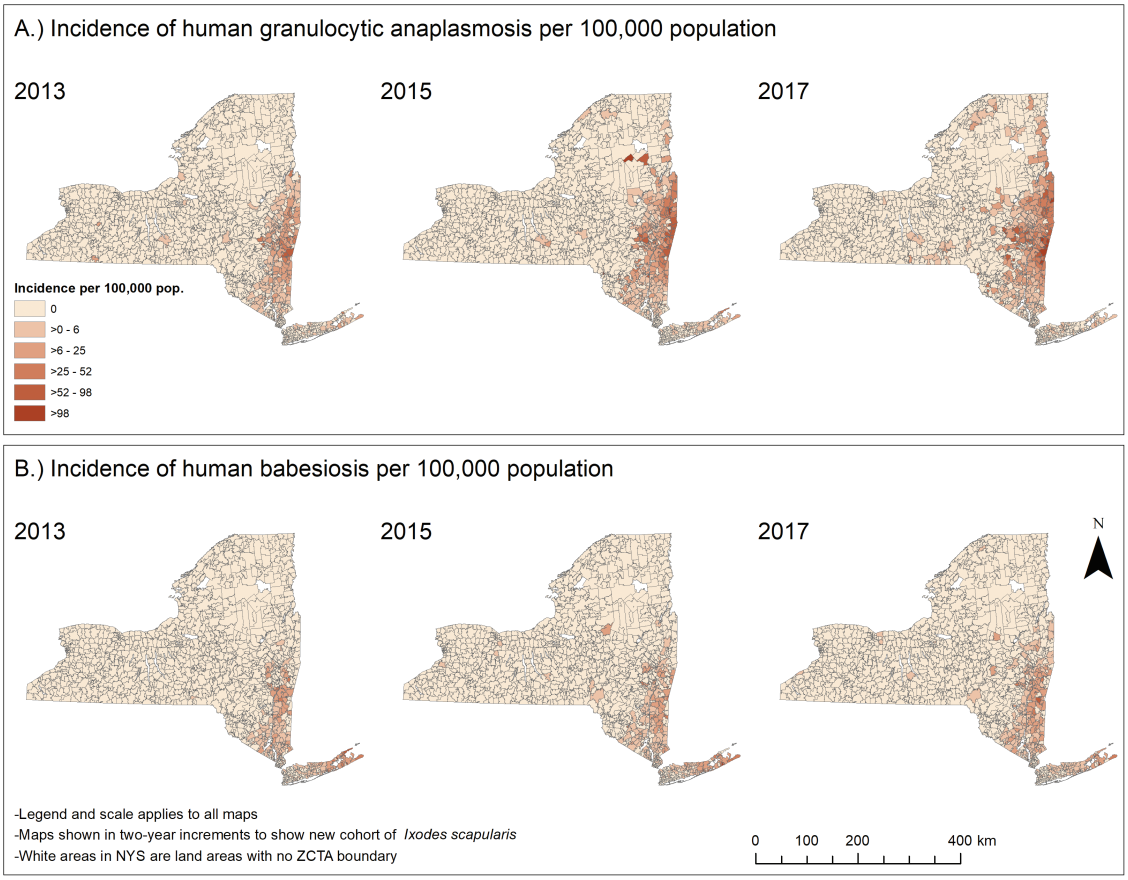

Fig. 2. Incidence of human granulocytic anaplasmosis and human babesiosis per 100,000 individuals aggregated to zip code tabulation area in NYS excluding New York City (2013, 2015, and 2017).

pathogen are exhibited (Fig. 4). Results indicated 145 sites where no *A. phagocytophilum*-infected *I. scapularis* had been collected and 203 sites where no *B. microti*-infected *I. scapularis* had been collected. The number of sites with specific pathogen infections among *I. scapularis* before 2013 or on initial site visits were 98 for *A. phagocytophilum* and 49 for *B. microti*. The number of sites with specific pathogen infections occurring on or after 2013 were 76 for *A. phagocytophilum* and 67 for *B. microti*.

The 319 field collection sites were contained within 240 of 1,582 ZCTAs (15.17%). Of the 240 ZCTAs with field collection sites, the mean and median number of sites per ZCTA were 1.33 and 1.00 respectively. The number of collection sites contained by a single ZCTA ranged from zero to four. Three ZCTAs (0.19%) contained four collection sites, 11 ZCTAs (0.70%) contained three collection sites, 48 ZCTAs (3.03%) contained two collection sites, and 178 ZCTAs contained one collection site (11.25%).

Violin plots showing the distribution of incidence for each disease among the three site categories and their respective Kruskal–Wallis and pairwise Wilcoxon rank sum tests ($\alpha = 0.05$) are shown (Fig. 5 and Table 2). Results of violin plots indicate HGA and human babesiosis incidence at ZCTA level generally increase due to the presence of *A. phagocytophilum* and *B. microti* in *I. scapularis* from surrounding environments. Further, the violin plots show an earlier appearance of *A. phagocytophilum* and *B. microti* within *I. scapularis* populations in the nearby environment results in a higher incidence of both HGA and human babesiosis.

Zero-Inflated Negative Binomial Regression of Environmental Factors on Cases of Human Granulocytic Anaplasmosis and Human Babesiosis

Examining the environmental covariates using a correlation matrix indicated that many covariates were highly correlated. Specific variables excluded from ZINB regression analysis due to high correlation were mean dewpoint temperature, mean temperature, maximum vapor pressure deficit, minimum vapor pressure deficit, and maximum temperature. Following exclusions, the remaining variables examined via ZINB modeling were mean elevation, percent forest cover, percent forest land cover change, percent urban land cover change, winter precipitation, and winter minimum temperature.

Following initial ZINB model building procedures, Moran's I of the residuals from the non-spatially controlled models provided evidence for spatial heterogeneity in both the HGA model ($z = 9.22$; $I = 1.37$; $P < 0.001$) and human babesiosis model ($z = 9.22$; $I = 1.38$; $P < 0.001$). In both the HGA and human babesiosis models, the autocovariate was significant in both the negative binomial and zero-inflated portions of the models. When comparing the AIC between the spatially adjusted and unadjusted HGA and human babesiosis models, the AICs were 607.61 and 223.92 points lower, respectively. Due to the decreases in AIC when accounting for spatial heterogeneity, the autocovariate terms were included in both the count and zero-inflated portions of the HGA and human babesiosis final models. Results for final spatially-weighted ZINB regression models for HGA and human babesiosis are shown in Table 3.

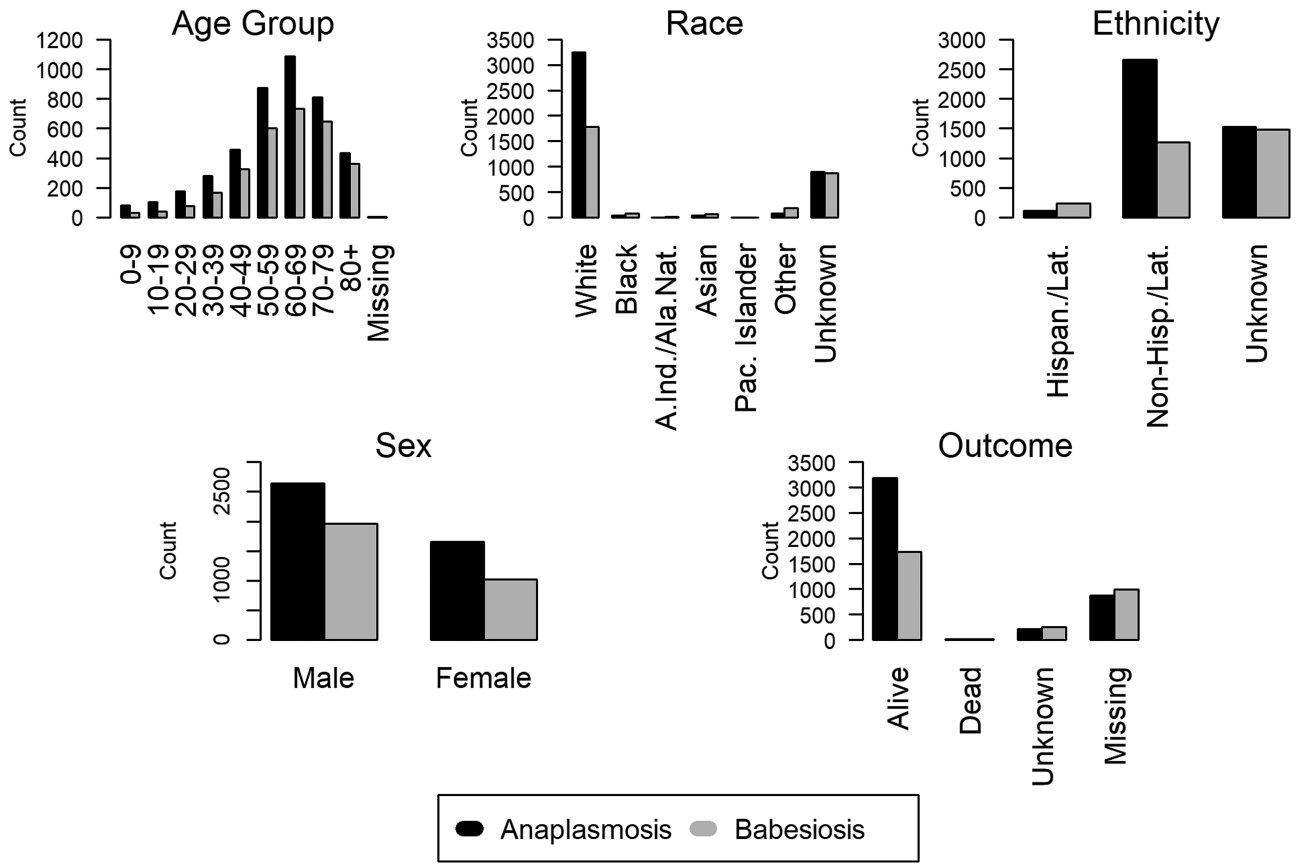

Fig. 3. Frequency distributions of demographic characteristics of human granulocytic anaplasmosis and human babesiosis cases in New York State (2013–2018).

Discussion

This study describes variations in the epidemiological and spatial risk of HGA and human babesiosis, two tick-borne diseases spread by the same tick vector (Spielman et al. 1979, Chen et al. 1994, Dumler et al. 2001) and maintained in the environment in the same major reservoir (Healy et al. 1976, Spielman et al. 1981, Telford and Spielman 1993, Telford et al. 1996, Hersh et al. 2012, Keesing et al. 2012, Stafford et al. 2014, Stephenson and Foley 2016) across NYS. This study also establishes the influence that climate, weather, and landscape characteristics have on the incidence of HGA and human babesiosis. Although this study did not use time-series data to examine the change of climate across NYS, the spatial variation of climate, weather, and landscape characteristics across NYS geography can be used to determine areas in NYS that are more susceptible to the encroachment of disease and the overall increase of disease risk.

Epidemiological analysis of demographic distributions for age, sex, race, and ethnicity showed similar trends between HGA and human babesiosis. Both diseases mostly impacted individuals above the age of 50 yr old, individuals who were male, individuals who were white, and individuals who were non-Hispanic and non-Latino, which is consistent with the current literature on tick-borne diseases (White et al. 1998; Dahlgren et al. 2011, 2015; Schwartz et al. 2017). Individuals in the race categories of Black, Asian, other, and unknown had a higher incidence of human babesiosis than HGA. Human babesiosis surveillance data also showed a higher percentage of cases of unknown ethnicity than HGA. The slight differences in race and ethnicity between HGA and human babesiosis could be a result of the geographic difference in the spread of each disease in NYS. Fig. 4 shows that human babesiosis incidence is higher in the more racially diverse region of Long Island, while HGA incidence is higher in the less racially diverse upper Hudson Valley region (United States Census Bureau 2013).

The violin plots in Fig. 5 show that the presence of a pathogen in the environment shifted the number of ZCTAs away from the first bimodal peak centered around zero cases of disease towards the second bimodal peak centered around non-zero cases of the disease. Additionally, the earlier the pathogen presented in the environment resulted in a further increase in the incidence of disease shown by the increase in the mean value of incidence. Interestingly, the results of the pairwise Wilcoxon rank sum tests (Table 2) indicate that finding *A. phagocytophilum* within a ZCTA before or after 2013 had no statistically significant effect on the distribution of HGA incidence. The lack of a statistical difference in the distribution of HGA between the two different temporal pathogen emergence groups could be due to the inability of the PCR assays utilized to differentiate between two predominant pathogenic and nonpathogenic genetic variants of *A. phagocytophilum*. The variant Ap-v1 does not cause disease in humans (Massung, Priestley, et al. 2003) and has a primary reservoir of white-tailed deer (*Odocoileus virginianus* Zimmermann (Artiodactyla: Cervidae)) (Massung et al. 2005), while the variant Ap-ha is pathogenic to humans (Massung, Mather et al. 2003) and has reservoirs of white-footed mice (*Peromyscus leucopus*) and Eastern chipmunks (*Tamias striatus* L. (Rodentia: Cricetidae)) (Keesing et al. 2014). Studies in Ontario, Canada show a shift in the proportion of *A. phagocytophilum* infections in *I. scapularis* toward the Ap-ha variant and away from the Ap-v1 variant when comparing the populations before and after 2010 (Krakowetz et al. 2014, Werden et al. 2015, Nelder et al.

Table 1. Demographic distributions and weighted incidence rates per 100,000 of human granulocytic anaplasmosis (HGA) and human babesiosis in New York State (2013–2018)

	HGA	Incidence per 100,000	Human babesiosis	Incidence per 100,000
	(*n* = 4297)		(*n* = 2986)	
Age (years)				
0–9	80 (1.86%)	1.02	31 (1.04%)	0.39
10–19	102 (2.37%)	1.09	38 (1.27%)	0.41
20–29	176 (4.09%)	2.04	77 (2.58%)	0.89
30–39	281 (6.54%)	3.67	168 (5.63%)	2.20
40–49	458 (10.66%)	4.68	326 (10.92%)	3.33
50–59	873 (20.32%)	8.75	602 (20.16%)	6.03
60–69	1084 (25.23%)	15.43	732 (24.51%)	10.42
70–79	808 (18.80%)	20.24	648 (21.70%)	16.24
80+	433 (10.08%)	14.24	362 (12.12%)	11.91
Missing	2 (0.05%)	–	2 (0.07%)	–
Age (years)				
Mean (SD)	58.49 (18.20)	–	61.00 (16.72)	–
Median [Min, Max.]	61.00 (<1.0,101)	–	63.00 (<1.0,99)	–
Sex				
Male	2638 (61.39%)	7.98	1963 (65.74%)	5.94
Female	1659 (38.61%)	4.84	1023 (34.26%)	2.99
Race				
White	3244 (75.49%)	5.93	1786 (59.81%)	3.26
Black	34 (0.79%)	0.58	82 (2.75%)	1.39
American Indian/Alaska Native	1 (0.02%)	0.41	5 (0.17%)	2.07
Asian	35 (0.82%)	1.45	66 (2.21%)	2.74
Pacific Islander	1 (0.02%)	5.63	4 (0.13%)	22.51
Other	81 (1.89%)	2.02	177 (5.93%)	4.42
Unknown	901 (20.97%)	–	866 (29.00%)	–
Ethnicity				
Hispanic or Latino	107 (2.48%)	0.18	234 (7.84%)	0.39
Non-Hispanic/Non-Latino	2659 (61.88%)	39.68	1267 (42.31%)	18.91
Unknown	1531 (35.63%)	–	1485 (49.73%)	–
Outcome				
Alive	263 (6.12%)	–	363 (12.16%)	–
Dead	15 (0.35%)	–	12 (0.40%)	–
Unknown	3141 (73.10%)	–	1617 (54.15%)	–
Missing	878 (20.43%)	–	994 (33.29%)	–

2019). As Ontario neighbors NYS, it is plausible that populations of *I. scapularis* in NYS are exhibiting a similar shift in population dynamics. This phenomenon would result in the mischaracterization of collection sites, and in turn, bias the result of the Wilcoxon rank-sum test towards the null hypothesis. Fig. 4 illustrates this effect, as it shows collection sites throughout NYS that have had positive PCR results for *A. phagocytophilum* in *I. scapularis*, while also exhibiting low to zero incidence of HGA in their respective ZCTAs. Collection sites with *B. microti*-infected *I. scapularis* are less widespread in NYS compared to HGA, and the presence/absence of cases of human babesiosis at the ZCTA level seem to follow the spatial trend of pathogen presence/absence. Another potential limitation in comparing PCR results from field collection sites to the incidence of disease at the ZCTA level is the varying spatial and temporal sample size. Not all ZCTAs contained an equal number of field collection sites, and not all field collection sites were visited at the same frequency. ZCTAs were coded according to the temporal appearance of a specific pathogen as opposed to the prevalence of pathogen-positive *I. scapularis*. Thus, ZCTAs with visits at different sites and a greater frequency of visits at sites are more likely to detect a pathogen, if present in the environment. However, spatial and temporal trends are still notable.

ZINB regression models provided the means to compare how HGA and human babesiosis are affected by climate and landscape characteristics. The two-part modeling process using a count and zero-inflated model requires variables from ZINB models to be interpreted as either "consonant" (the direction of association between the predictor variable and outcome variable is the same in both parts of the model), "dissonant" (the direction of association is different in both parts of the model and "neutral" (a variable is only statistically significant in one part of the model) (Lachenbruch 2001, Xu et al. 2015). Variables with consonant trends in the HGA model included elevation and percent mixed/deciduous forest cover, while the human babesiosis model's only consonant variable was percent mixed/deciduous forest cover. Variables with dissonant trends in the HGA model included percent urban land cover change and minimum winter temperature, while the human babesiosis model's only dissonant variable was minimum winter temperature. All remaining variables in both models were considered neutral.

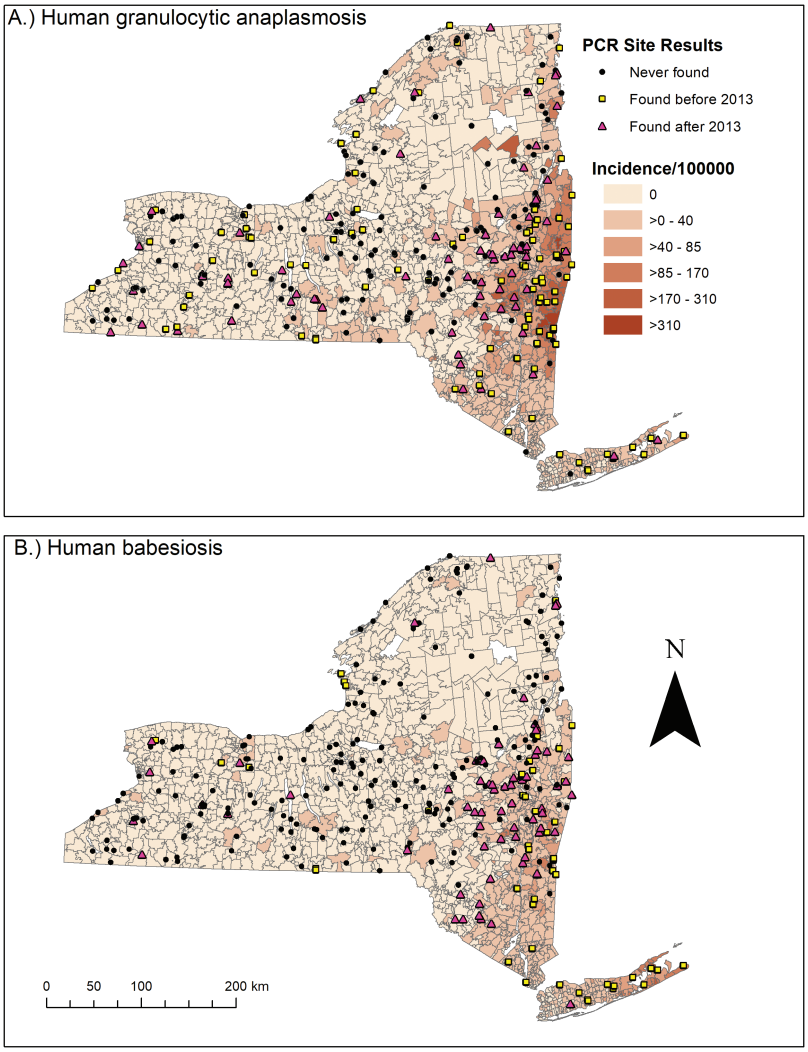

Fig. 4. Map of NYS with the incidence of human granulocytic anaplasmosis and human babesiosis per 100,000 population by zip code tabulation area (2013–2018), overlaid with tick collection site locations categorized by temporal pathogen emergence of *Anaplasma phagocytophilum* and *Babesia microti*.

Elevation was negatively associated with the magnitude of cases in the HGA [IRR = 0.52, 95% CI = 0.50–0.54] and human babesiosis models [IRR = 0.37, 95% CI = 0.34–0.40], which is in agreement with current literature regarding Lyme disease (Arab 2015) and tick density (Gilbert 2010, Hahn et al. 2016, Allen et al. 2019). The negative association between elevation and both HGA and human babesiosis in NYS is likely due to a combination of environmental and ecological factors. Generally, mean temperatures are lower at higher elevations (Fig. 6), decreasing *I. scapularis* questing and development rates (Gilbert 2010). Further, white-tailed deer tend to congregate at lower elevations, depriving adult-stage *I. scapularis* at higher elevations of its primary reproductive host (Hurst and Porter 2008, Gilbert 2010). Elevation was positively associated with being a structural zero in the zero-inflated portion of the HGA model [OR = 2.04, 95% CI = 1.74–2.40], which agrees with the findings of Diuk Wasser et al (2010).

The percent of a ZCTA covered by mixed/deciduous forest was positively associated with HGA [IRR = 1.49, 95% CI = 1.45–1.52] and human babesiosis [IRR = 1.56, CI = 1.52–1.60] in the count portions of each model. The percent mixed/deciduous forest variable was negatively associated with being a structural zero case of HGA [OR = 0.55, 95% CI = 0.49–0.61] and human babesiosis [OR = 0.57, 95% CI = 0.49–0.66]. Deciduous forests are the preferred habitat for *I. scapularis* and their hosts (Frank et al. 1998), and thus, ZCTAs that are more covered by these forest types provide an increased risk for tick encounters (Brownstein, Skelly et al. 2005).

Land cover change may have varying effects on the risk for tick-borne disease due to fluctuations in *I. scapularis* and *P. leucopus* populations (Ostfeld and Keesing 2000) as well as the creation of forest edge (Brownstein, Skelly et al. 2005, Berl et al. 2018). The results of the ZINB models showed significant associations with both the forest and urban land cover change variables, but the interpretability of the results are limited due to the structure of the NLCD 2016 Land Cover Change Index data. The NLCD 2016 Land Cover Change Index combines the designation of areas that changed either to or from specific land cover classes during the period of 2001 to 2016, which presents a significant barrier in determining the exact effect that specific land cover changes have. The count portions of the final models showed an increase in the percent of a ZCTA that changed to or from forest land cover increased the risk for HGA [IRR = 10.11, 95% CI = 7.38–13.85] and human babesiosis [IRR = 6.13, 95% CI = 4.15–9.07], which agrees with current literature (Piedmonte et al. 2018). Percent urban land cover change has a negative association with the magnitude of cases of HGA in the

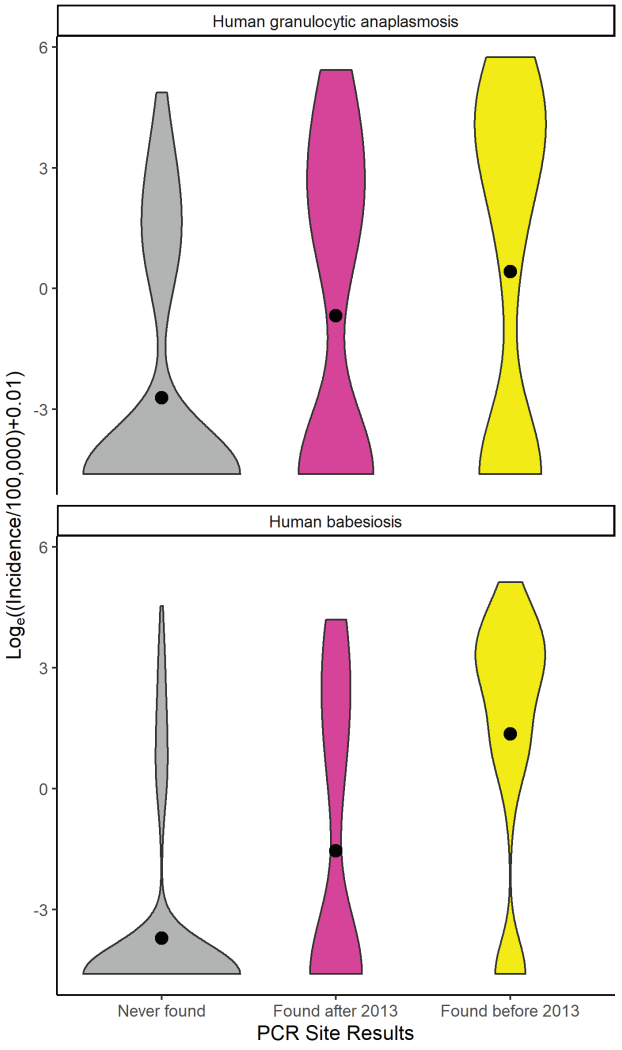

Fig. 5. Violin plots comparing temporal emergence of disease-causing pathogen at collection sites and respective incidence of human disease per 100,000 population at zip code tabulation area level (2013–2018). Black circles correspond to the mean incidence of human granulocytic anaplasmosis and human babesiosis at zip code tabulation area level.

Table 2. Results of Kruskal–Wallis test and pairwise Wilcoxon rank sum tests on mean incidence of human granulocytic anaplasmosis and human babesiosis (2013–2018) for categories of respective pathogen emergence

Pairwise Wilcoxon test	Kruskal–Wallis test:		0.001
Anaplasma phagocytophilum sites:			
Site Category:	**1**	**2**	**3**
1. No PCR positives	X		
2. PCR positives found before 2013	0.001	X	
3. PCR positives found after 2013	<0.001	0.057	X
Babesia microti sites:	Kruskal–Wallis test:		0.001
Site Category:	**1**	**2**	**3**
1. No PCR positives	X		
2. PCR positives found before 2013	<0.001	X	
3. PCR positives found after 2013	<0.001	<0.001	X

count portion of the model [IRR = 0.38, 95% CI = 0.32–0.44], while the odds of being a structural zero are negatively associated with urban land cover change for both HGA [OR = 0.23, 95% CI = 0.08–0.066] and human babesiosis [OR = 0.24, 95% CI = 0.08–0.066]. It is likely that the inability to differentiate between a change to or from the urban land cover classes is driving the dissonant and neutral effects in the HGA and human babesiosis models, respectively. New data that separates the land cover class designations by direction of change may help elucidate the dissonant and neutral effects of both the HGA and human babesiosis models.

Minimum temperature was used to estimate the effect that low temperatures have on *I. scapularis* populations infected with both *A. phagocytophilum* and *B. microti*. Neelankata et al. (2010) showed that *I. scapularis* infected with *A. phagocytophilum* express the *iafgp* gene, which encodes an antifreeze glycoprotein that allows *I. scapularis* to be active at and survive better in colder temperatures (Neelakanta et al. 2010). However, the effect of *iafgp* expression on *I. scapularis* overwintering survival in nature has not been demonstrated. The count portions of both final models exhibited a negative association with minimum winter temperature and case counts of HGA [IRR = 0.54, 95% CI = 0.51–0.57] and human babesiosis [IRR = 0.77, 95% CI = 0.71–0.82]. The IRRs of both count models showed that lower minimum winter temperatures resulted in a relatively larger increase of HGA cases than human babesiosis cases in NYS between 2013 and 2018. This relationship may partly be explained by the expression of the *iafgp* gene, allowing HGA incidence to increase in more northern latitudes. The zero-inflated portions of both the HGA [OR = 0.75, 95% CI = 0.65–0.87] and human babesiosis [OR = 0.39, 95% CI = 0.32–0.48] models exhibited a dissonant effect, likely because the coldest temperatures in the mountainous Adirondack region exhibit zero cases of both diseases (Figs. 4 and 6).

Winter precipitation was only significant in the count portions of both models, where it was negatively associated with HGA case counts [IRR = 0.97, 95% CI = 0.96–0.98] and positively associated with human babesiosis case counts [IRR = 1.12, 95% CI = 1.09–1.14]. The opposing directionality of effects in each count model may be due to the higher winter precipitation on Long Island, a location with generally lower snowfall than Upstate New York. PRISM does not have snowfall data available, thus, mean precipitation from November to March was used to estimate mean winter snowfall, likely including rainfall in areas where snow is less common. In areas with colder temperatures, *I. scapularis* dormant under the winter snow and are insulated from adverse fluctuations in temperature and humidity (Eisen et al. 2016, Linske et al. 2019). Due to the insulating effects of snow, it is possible the effect of snowfall on rates of disease would differ across levels of minimum winter temperatures. That is, in areas where minimum winter temperatures are low, an increase in snowfall would likely result in an increase in *I. scapularis* over-winter survival, while in areas where minimum winter temperatures and humidity are higher, such as the maritime climate of Long Island, the effect of snow on tick survivability may be negligible. Future studies should aim to examine only snowfall, and potential effect modification with minimum winter temperatures.

The limitations of this study are evident in the general interpretability of the results. Some variables examined are not specific enough to make inference on the cause–effect relationship between environment and disease, while others are clouded by the focality of higher rates of disease when compared to statewide environmental conditions. Additionally, some variables were excluded from the start of the analysis due to high correlation, which is expected in a study examining the magnitude and direction of specific environmental variables on rates of disease. Another limitation stems from

Table 3. Final zero-inflated negative binomial regression models of environmental covariates and case counts of human granulocytic anaplasmosis (HGA) and human babesiosis

HGA						Human babesiosis					
	IRR	95% CI	SE	*z*-value	*P*		IRR	95% CI	SE	*z*-value	*P*
Negative Binomial						Negative Binomial					
Intercept	0.00	0.00–0.00	0.61	−35.54	<0.001	Intercept	0.00	0.00–0.00	0.92	−19.23	<0.001
Mean elevation (m)[a]	0.52	0.50–0.54	0.02	−31.89	<0.001	Mean elevation (m)[a]	0.37	0.34–0.40	0.04	−26.15	<0.001
Percent forest cover[b]	1.49	1.45–1.52	0.01	35.65	<0.001	Percent forest cover[b]	1.56	1.52–1.60	0.01	33.40	<0.001
Percent forest land cover change[b]	10.11	7.38–13.85	0.16	14.42	<0.001	Percent forest land cover change[b]	6.13	4.15–9.07	0.20	9.10	<0.001
Percent urban land cover change[b]	0.38	0.32–0.44	0.08	−11.54	<0.001	Mean winter preciptitation (cm)[b]	1.12	1.09–1.14	0.01	9.94	<0.001
Mean winter preciptitation (cm)[b]	0.97	0.96–0.98	0.01	−4.04	<0.001	Mean winter minimum temperature (°C)	0.77	0.71–0.82	0.04	−7.14	<0.001
Mean winter minimum temperature (°C)	0.54	0.51–0.57	0.02	−24.92	<0.001	Autocovariate	1.00	1.00–1.00	0.00	15.02	<0.001
Autocovariate	1.00	1.00–1.00	0.00	26.05	<0.001						
	OR	95% CI	SE	*z*-value	*P*		OR	95% CI	SE	*z*-value	*P*
Logit						Logit					
Intercept	0.01	0.00–0.11	13.78	−3.42	0.001	Intercept	0.00	0.00–0.00	1.91	−9.26	<0.001
Mean elevation (m)[a]	2.04	1.74–2.40	0.08	8.70	<0.001	Percent forest cover[b]	0.57	0.49–0.66	0.08	−7.36	<0.001
Percent forest cover[b]	0.55	0.49–0.61	0.06	−10.41	<0.001	Percent urban land cover change[b]	0.24	0.08–0.66	0.52	−2.74	0.006
Percent urban land cover change[b]	0.23	0.08–0.66	0.54	−2.73	0.006	Mean winter minimum temperature (°C)	0.39	0.32–0.48	0.10	−9.39	<0.001
Mean winter minimum temperature (°C)	0.75	0.65–0.87	0.77	−3.72	<0.001	Autocovariate	1.00	1.00–1.00	0.00	−3.71	<0.001
Autocovariate	1.00	1.00–1.00	0.00	−5.15	<0.001						

[a]Variable divided by 100 for interpretability, one unit in table is equal to 100 units.
[b]Variable divided by 10 for interpretability, one unit in table is equal to 10 units.

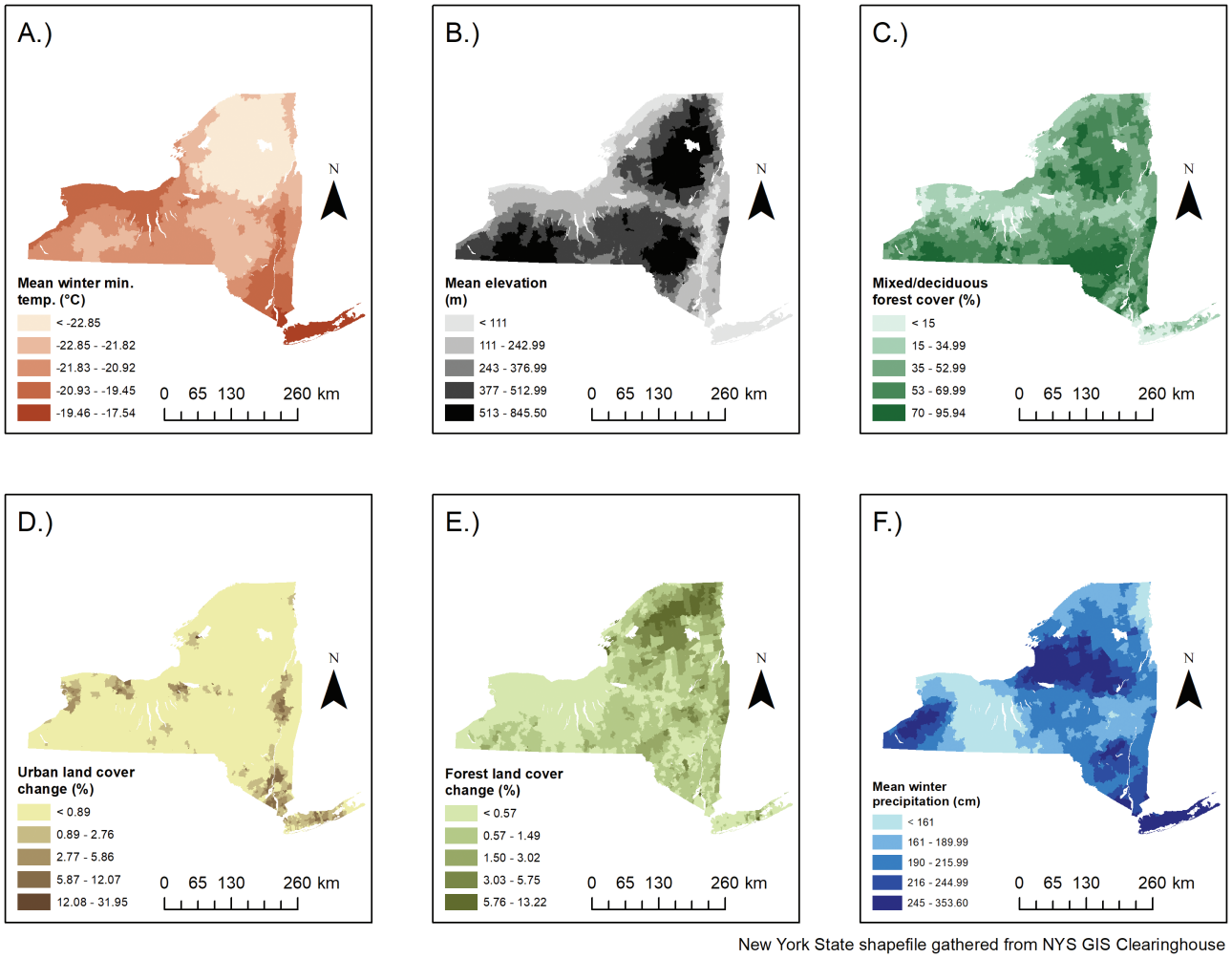

Fig. 6. Environmental covariates with statistically significant associations to either human granulocytic anaplasmosis or human babesiosis. A – Mean winter minimum temperature; B – Mean elevation; C – Percent mixed/deciduous forest cover; D – Percent urban land cover change; E – Percent forest land cover change; F – Mean winter precipitation.

HGA and human babesiosis being understudied compared to Lyme disease. The CDC estimates the true number of Lyme disease cases can be ten-fold higher than what is currently reported (Centers for Disease Control and Prevention 2013). Similar estimates are not available for HGA and human babesiosis, where if the magnitude of underreporting is relatively different between the two, bias could be introduced.

The association that NYS climate, weather, and landscape features have with HGA and human babesiosis is complex and understudied. Scientific studies on tick-borne diseases generally examine the relationship of the environment with rates of Lyme disease or tick population density irrespective of pathogen prevalence. It is important to note that not all tick-borne diseases have the same scope, and the pathogens that infect *I. scapularis* have different ecological dynamics and spatial extents. As tick-borne disease cases continue to rise, the scientific community should attempt to elucidate the impact that the environment has on each tick-borne disease individually, to better guide disease-specific prevention policies and public education efforts.

Supplementary Data

Supplementary data are available at *Journal of Medical Entomology* online.

Acknowledgments

We would like to express their gratitude to the New York State Department of Environmental Conservation, the New York State Department of Parks, Recreation and Historic Preservation, and various county, town, and village park managers for granting us use of lands to conduct this research. We extend thanks to the following individuals for their assistance in collection, identification, and/or molecular testing of ticks: the students of Paul Smith's College, Jake Sporn and the boat launch stewards of the Adirondack Watershed Institute, Brian Leydet, Samantha Lanthier, NYSDOH employees and student interns: Lauren Rose, Anna Perry, Joshua Rosansky, Konrad Fondrie, Kaitlin Driesse, Michael Suatoni, Margaret Mahoney, Michelle Wemette, Sandra Beebe, Kayla Mehigan, Emily Haner, Franz Soiro, Katherine Guilbo, Samantha Sandwick, Morgan Thorne, Kate Turcotte, Jacob Miller, Joseph Prusinski Jr., Jennifer DeLorenzo, Lauren DeLorenzo, James Sherwood, John Howard, Rachel Reichel, Ariel Robinson, Marly Katz, Adam Rowe, Jean Stella, Donald Campbell, Daniella Giardina, Melissa Stone, Thomas Mistretta, R.C. Rizzitello, Emily Gicewicz, Christopher Murphy, David Rice, Nicholas Piedmonte, Melissa Fierke and associates with the State University of New York (SUNY) College of Environmental Science and Forestry, Colgate University students and faculty, Claire Hartl and others from SUNY Brockport, Niagara County DOH, Erie County DOH, Cornell Cooperative Extension of Onondaga County, Scott Campbell, Michael Santoriello, Christopher Romano and Suffolk County DOH, and Ilia Rochlin and Moses Cucura and Suffolk County Vector Control. This work was supported by the NYSDOH, the National Institutes of Health (grants AI097137, AI142572), and the Centers

for Disease Control and Prevention (award U01CK000509). The content is solely the responsibility of the authors and does not necessarily represent the official views of the National Institutes of Health or the Centers for Disease Control and Prevention.

References Cited

Allen, D., B. Borgmann-Winter, L. Bashor, and J. Ward. 2019. The density of the Lyme disease vector Ixodes scapularis (Blacklegged Tick) differs between the Champlain Valley and Green Mountains, Vermont. Northeast. Nat. 23: 545–560.

Arab, A. 2015. Spatial and spatio-temporal models for modeling epidemiological Data with excess zeros. Int. J. Environ. Res. Public Health. 12: 10536–10548.

Ashley, S., and V. Meentemeyer. 2004. Climatic analysis of Lyme disease in the United States. Clim. Res. 27: 177–187.

Bakken, J. S., J. Krueth, C. Wilson-Nordskog, R. Tilden, K. Asanovich, and S. Dumler. 1996. Clinical and laboratory characteristics of human granulocytic ehrlichiosis. J. Am. Med. Assoc. 275: 199–205.

Berger, K. A., H. S. Ginsberg, K. D. Dugas, L. H. Hamel, and T. N. Mather. 2014. Adverse moisture events predict seasonal abundance of Lyme disease vector ticks (Ixodes scapularis). Parasit. Vectors. 7: 181.

Berger, K. A., H. S. Ginsberg, L. Gonzalez, and T. N. Mather. 2014. Relative humidity and activity patterns of Ixodes scapularis (Acari: Ixodidae). J. Med. Entomol. 51: 769–776.

Berl, J. L., K. F. Kellner, E. A. Flaherty, and R. K. Swihart. 2018. Spatial variation in density of white-footed mice along edges in fragmented habitat. Am. Midl. Nat. 179: 38–50.

Bhowmik, K. R., S. Das, and M. A. Islam. 2020. Modelling the number of antenatal care visits in Bangladesh to determine the risk factors for reduced antenatal care attendance. PLoS One. 15: e0228215.

Bivand, R. S., and D. W. S. Wong. 2018. Comparing implementations of global and local indicators of spatial association. TEST. 27: 716–748.

Brownstein, J. S., T. R. Holford, and D. Fish. 2003. A climate-based model predicts the spatial distribution of the Lyme disease vector Ixodes scapularis in the United States. Environ. Health Perspect. 111: 1152–1157.

Brownstein, J. S., T. R. Holford, and D. Fish. 2005. Effect of climate change on Lyme disease risk in North America. Ecohealth. 2: 38–46.

Brownstein, J. S., D. K. Skelly, T. R. Holford, and D. Fish. 2005. Forest fragmentation predicts local scale heterogeneity of Lyme disease risk. Oecologia. 146: 469–475.

Burtis, J. C., P. Sullivan, T. Levi, K. Oggenfuss, T. J. Fahey, and R. S. Ostfeld. 2016. The impact of temperature and precipitation on blacklegged tick activity and Lyme disease incidence in endemic and emerging regions. Parasit. Vectors. 9: 606.

Centers for Disease Control and Prevention. 2013. CDC provides estimate of Americans diagnosed with Lyme disease each year. https://www.cdc.gov/media/releases/2013/p0819-lyme-disease.html

Chamberlain, A. M., S. M. Dunlay, Y. Gerber, S. M. Manemann, R. Jiang, S. A. Weston, and V. L. Roger. 2017. Burden and timing of hospitalizations in heart failure: a community study. Mayo Clin. Proc. 92: 184–192.

Chen, S. M., J. S. Dumler, J. S. Bakken, and D. H. Walker. 1994. Identification of a granulocytotropic Ehrlichia species as the etiologic agent of human disease. J. Clin. Microbiol. 32: 589–595.

Council of State and Territorial Epidemiologists. 2008. Ehrlichiosis and anaplasmosis 2008 case definition. (https://wwwn.cdc.gov/nndss/conditions/ehrlichiosis-and-anaplasmosis/case-definition/2008/).

Council of State and Territorial Epidemiologists. 2011. Babesiosis (Babesia spp.) 2011 Case Definition. (https://wwwn.cdc.gov/nndss/conditions/babesiosis/case-definition/2011/).

Dahlgren, F. S., K. N. Heitman, N. A. Drexler, R. F. Massung, and C. B. Behravesh. 2015. Human granulocytic anaplasmosis in the United States from 2008 to 2012: a summary of national surveillance data. Am. J. Trop. Med. Hyg. 93: 66–72.

Dahlgren, F. S., E. J. Mandel, J. W. Krebs, R. F. Massung, and J. H. McQuiston. 2011. Increasing incidence of Ehrlichia chaffeensis and Anaplasma phagocytophilum in the United States, 2000–2007. Am. J. Trop. Med. Hyg. 85: 124–131.

Daniels, T. J., T. M. Boccia, S. Varde, J. Marcus, J. Le, D. J. Bucher, R. C. Falco, and I. Schwartz. 1998. Geographic risk for Lyme disease and human granulocytic ehrlichiosis in southern New York state. Appl. Environ. Microbiol. 64: 4663–4669.

Danielson, J. J., and D. B. Gesch. 2011. Global multi-resolution terrain elevation data 2010 (GMTED2010). U.S. Geological Survey Open-File Report 2011-1073, 1-26.

Dennis, D. T., T. S. Nekomoto, J. C. Victor, W. S. Paul, and J. Piesman. 1998. Reported distribution of Ixodes scapularis and Ixodes pacificus (Acari: Ixodidae) in the United States. J. Med. Entomol. 35: 629–638.

Diuk-Wasser, M. A., A. G. Hoen, P. Cislo, R. Brinkerhoff, S. A. Hamer, M. Rowland, R. Cortinas, G. Vourc'h, F. Melton, G. J. Hickling, et al. 2012. Human risk of infection with Borrelia burgdorferi, the Lyme disease agent, in Eastern United States. Am. J. Trop. Med. Hyg. 86: 320–327.

Diuk-Wasser, M. A., G. Vourc'h, P. Cislo, A. G. Hoen, F. Melton, S. A. Hamer, M. Rowland, R. Cortinas, G. J. Hickling, J. I. Tsao, et al. 2010. Field and climate-based model for predicting the density of host-seeking nymphal Ixodes scapularis, an important vector of tick-borne disease agents in the eastern United States. Glob. Ecol. Biogeogr. 19: 504–514.

Dumler, J. S., A. F. Barbet, C. P. Bekker, G. A. Dasch, G. H. Palmer, S. C. Ray, Y. Rikihisa, and F. R. Rurangirwa. 2001. Reorganization of genera in the families Rickettsiaceae and Anaplasmataceae in the order Rickettsiales: unification of some species of Ehrlichia with Anaplasma, Cowdria with Ehrlichia and Ehrlichia with Neorickettsia, descriptions of six new species combinations and designation of Ehrlichia equi and "HGE agent" as subjective synonyms of Ehrlichia phagocytophila. Int. J. Syst. Evol. Microbiol. 51: 2145–2165.

Dunn, O. J. 1964. Multiple comparisons using rank sums. Technometrics. 6: 241–252.

Eisen, R. J., L. Eisen, N. H. Ogden, and C. B. Beard. 2016. Linkages of weather and climate with Ixodes scapularis and Ixodes pacificus (Acari: Ixodidae), enzootic transmission of Borrelia burgdorferi, and Lyme disease in North America. J. Med. Entomol. 53: 250–261.

ESRI. 2018. ArcMap. ESRI, Redlands, California. USA.

ESRI. 2019. Spatial Analyst Tools. ESRI, Redlands, California. USA.

F. Dormann, C., J. M. McPherson, M. B. Araújo, R. Bivand, J. Bolliger, G. Carl, R. G. Davies, A. Hirzel, W. Jetz, W. Daniel Kissling, et al. 2007. Methods to account for spatial autocorrelation in the analysis of species distributional data: a review. Ecography. 30: 609–628.

Frank, D. H., D. Fish, and F. H. Moy. 1998. Landscape features associated with Lyme disease risk in a suburban residential environment. Landsc. Ecol. 13: 27–36.

Gall, C. A., K. E. Reif, G. A. Scoles, K. L. Mason, M. Mousel, S. M. Noh, and K. A. Brayton. 2016. The bacterial microbiome of Dermacentor andersoni ticks influences pathogen susceptibility. ISME J. 10: 1846–1855.

Gilbert, L. 2010. Altitudinal patterns of tick and host abundance: a potential role for climate change in regulating tick-borne diseases? Oecologia. 162: 217–225.

Guerra, M., E. Walker, C. Jones, S. Paskewitz, M. R. Cortinas, A. Stancil, L. Beck, M. Bobo, and U. Kitron. 2002. Predicting the risk of Lyme disease: habitat suitability for Ixodes scapularis in the north central United States. Emerg. Infect. Dis. 8: 289–297.

Hahn, M. B., C. S. Jarnevich, A. J. Monaghan, and R. J. Eisen. 2016. Modeling the geographic distribution of Ixodes scapularis and Ixodes pacificus (Acari: Ixodidae) in the contiguous United States. J. Med. Entomol. 53: 1176–1191.

Halos, L., S. Bord, V. Cotté, P. Gasqui, D. Abrial, J. Barnouin, H. J. Boulouis, M. Vayssier-Taussat, and G. Vourc'h. 2010. Ecological factors characterizing the prevalence of bacterial tick-borne pathogens in Ixodes ricinus ticks in pastures and woodlands. Appl. Environ. Microbiol. 76: 4413–4420.

Healy, G. R., A. Speilman, and N. Gleason. 1976. Human babesiosis: reservoir in infection on Nantucket Island. Science. 192: 479–480.

Hersh, M. H., M. Tibbetts, M. Strauss, R. S. Ostfeld, and F. Keesing. 2012. Reservoir competence of wildlife host species for Babesia microti. Emerg. Infect. Dis. 18: 1951–1957.

Hochberg, Y. 1988. A sharper Bonferroni procedure for multiple tests of significance. Biometrika. 75: 800–802.

Homer, M. J., I. Aguilar-Delfin, S. R. Telford, 3rd, P. J. Krause, and D. H. Persing. 2000. Babesiosis. Clin. Microbiol. Rev. 13: 451–469.

Homer, C., J. Dewitz, S. Jin, G. Xian, C. Costello, P. Danielson, L. Gass, M. Funk, J. Wickham, S. Stehman, et al. 2020. Conterminous United States land cover change patterns from 2001–2016 from the 2016 National Land Cover Database. ISPRS J. Photogramm. Remote Sens. 162: 184–199.

Hurst, J. E., and W. F. Porter. 2008. Evaluation of shifts in white-tailed deer winter yards in the Adirondack region of New York. J. Wildl. Manag. 72: 367–375.

Joseph, J. T., M. John, P. Visintainer, and G. P. Wormser. 2020. Increasing incidence and changing epidemiology of babesiosis in the Hudson Valley region of New York State: 2009–2016. Diagn. Microbiol. Infect. Dis. 96: 114958.

Joseph, J. T., S. S. Roy, N. Shams, P. Visintainer, R. B. Nadelman, S. Hosur, J. Nelson, and G. P. Wormser. 2011. Babesiosis in lower Hudson Valley, New York, USA. Emerg. Infect. Dis. 17: 843–847.

Keesing, F., M. H. Hersh, M. Tibbetts, D. J. McHenry, S. Duerr, J. Brunner, M. Killilea, K. LoGiudice, K. A. Schmidt, and R. S. Ostfeld. 2012. Reservoir competence of vertebrate hosts for Anaplasma phagocytophilum. Emerg. Infect. Dis. 18: 2013–2016.

Keesing, F., D. J. McHenry, M. Hersh, M. Tibbetts, J. L. Brunner, M. Killilea, K. LoGiudice, K. A. Schmidt, and R. S. Ostfeld. 2014. Prevalence of human-active and variant 1 strains of the tick-borne pathogen Anaplasma phagocytophilum in hosts and forests of eastern North America. Am. J. Trop. Med. Hyg. 91: 302–309.

Keirans, J. E., and C. M. Clifford. 1978. The genus Ixodes in the United States: a scanning electron microscope study and key to the adults. J. Med. Entomol. Suppl. 2: 1–149.

Keirans, J. E., H. J. Hutcheson, L. A. Durden, and J. S. Klompen. 1996. Ixodes (Ixodes) scapularis (Acari:Ixodidae): redescription of all active stages, distribution, hosts, geographical variation, and medical and veterinary importance. J. Med. Entomol. 33: 297–318.

Khatchikian, C. E., M. Prusinski, M. Stone, P. B. Backenson, I.-N. Wang, M. Z. Levy, and D. Brisson. 2012. Geographical and environmental factors driving the increase in the Lyme disease vector Ixodes scapularis. Ecosphere. 3: art85.

Kogut, S. J., C. D. Thill, M. A. Prusinski, J. H. Lee, P. B. Backerson, J. L. Coleman, M. Anand, and D. J. White. 2005. Babesia microti, upstate New York. Emerg. Infect. Dis. 11: 476–478.

Krakowetz, C. N., A. Dibernardo, L. R. Lindsay, and N. B. Chilton. 2014. Two Anaplasma phagocytophilum strains in Ixodes scapularis ticks, Canada. Emerg. Infect. Dis. 20: 2064–2067.

Kruskal, W. H., and W. A. Wallis. 1952. Use of ranks in one-criterion variance analysis. J. Am. Stat. Assoc. 47: 583–621.

Lachenbruch, P. A. 2001. Comparisons of two-part models with competitors. Stat. Med. 20: 1215–1234.

Linske, M. A., K. C. Stafford, S. C. Williams, C. B. Lubelczyk, M. Welch, and E. F. Henderson. 2019. Impacts of deciduous leaf litter and snow presence on nymphal Ixodes scapularis (Acari: Ixodidae) overwintering survival in coastal New England, USA. Insects. 10: 1–11.

Massung, R. F., J. W. Courtney, S. L. Hiratzka, V. E. Pitzer, G. Smith, and R. L. Dryden. 2005. Anaplasma phagocytophilum in white-tailed deer. Emerg. Infect. Dis. 11: 1604–1606.

Massung, R. F., T. N. Mather, R. A. Priestley, and M. L. Levin. 2003. Transmission efficiency of the AP-variant 1 strain of Anaplasma phagocytophila. Ann. N. Y. Acad. Sci. 990: 75–79.

Massung, R. F., R. A. Priestley, N. J. Miller, T. N. Mather, and M. L. Levin. 2003. Inability of a variant strain of Anaplasma phagocytophilum to infect mice. J. Infect. Dis. 188: 1757–1763.

Mekonnen, F. H., W. D. Lakew, Z. D. Tesfaye, and P. K. Swain. 2019. Statistical models for longitudinal zero-inflated count data: application to seizure attacks. Afr. Health Sci. 19: 2555–2564.

Moran, P. A. 1950. Notes on continuous stochastic phenomena. Biometrika. 37: 17–23.

Neelakanta, G., H. Sultana, D. Fish, J. F. Anderson, and E. Fikrig. 2010. Anaplasma phagocytophilum induces Ixodes scapularis ticks to express an antifreeze glycoprotein gene that enhances their survival in the cold. J. Clin. Invest. 120: 3179–3190.

Nelder, M. P., C. B. Russell, L. R. Lindsay, A. Dibernardo, N. C. Brandon, J. Pritchard, S. Johnson, K. Cronin, and S. N. Patel. 2019. Recent Emergence of Anaplasma phagocytophilum in Ontario, Canada: Early Serological and Entomological Indicators. Am. J. Trop. Med. Hyg. 101: 1249–1258.

New York State Department of Health. 2006a. Rate per 100,000 population – communicable disease in New York State – 2005. https://www.health.ny.gov/statistics/diseases/communicable/2005/rates1.htm

New York State Department of Health. 2006b. Communicable disease in New York State – reported cases by disease and county: AIDS – GIardiasis: 2000. https://www.health.ny.gov/statistics/diseases/communicable/2000/cases1.htm

New York State Department of Health. 2011. Rate per 100,000 population by disease and county: AIDS – Cyclospora (2010). https://www.health.ny.gov/statistics/diseases/communicable/2010/rates/1.htm

New York State Department of Health. 2018. Communicable disease in New York State – rate per 100,000 population of cases reported in 2018. New York State Department of Health.

New York State Department of Health. 2019. Communicable disease in New York State exclusive of New York City – rate per 100,000 of cases reported – 2009–2018 – for selected diseases. https://www.health.ny.gov/statistics/diseases/communicable/2018/docs/select_rates.pdf

Ogden, N. H., A. Maarouf, I. K. Barker, M. Bigras-Poulin, L. R. Lindsay, M. G. Morshed, C. J. O'callaghan, F. Ramay, D. Waltner-Toews, and D. F. Charron. 2006. Climate change and the potential for range expansion of the Lyme disease vector Ixodes scapularis in Canada. Int. J. Parasitol. 36: 63–70.

Ogden, N. H., L. St-Onge, I. K. Barker, S. Brazeau, M. Bigras-Poulin, D. F. Charron, C. M. Francis, A. Heagy, R. Lindsay, A. Maarouf, et al. 2008. Risk maps for range expansion of the Lyme disease vector, Ixodes scapularis, in Canada now and with climate change. Int. J. Health Geogr. 7: 24.

Ostfeld, R. S., and F. Keesing. 2000. Biodiversity and disease risk: the case of Lyme disease. Conserv. Biol. 14: 722–728.

Piedmonte, N. P., S. B. Shaw, M. A. Prusinski, and M. K. Fierke. 2018. Landscape features associated with blacklegged tick (Acari: Ixodidae) density and tick-borne pathogen prevalence at multiple spatial scales in Central New York State. J. Med. Entomol. 55: 1496–1508.

Preisser, J. S., J. W. Stamm, D. L. Long, and M. E. Kincade. 2012. Review and recommendations for zero-inflated count regression modeling of dental caries indices in epidemiological studies. Caries Res. 46: 413–423.

Prusinski, M. A., J. E. Kokas, K. T. Hukey, S. J. Kogut, J. Lee, and P. B. Backenson. 2014. Prevalence of Borrelia burgdorferi (Spirochaetales: Spirochaetaceae), Anaplasma phagocytophilum (Rickettsiales: Anaplasmataceae), and Babesia microti (Piroplasmida: Babesiidae) in Ixodes scapularis (Acari: Ixodidae) collected from recreational lands in the Hudson Valley Region, New York State. J. Med. Entomol. 51: 226–236.

R Core Team. 2019. R: A language and environment for statistical computing. R Foundation for Statistical Computing, Vienna, Austria.

Ramsey, A. H. 2002. Outcomes of treated human granulocytic Ehrlichiosis cases. Emerg. Infect. Dis. 8: 398–401.

Schloerke, B., J. Crowley, D. Cook, F. Briatte, M. Marbach, E. Thoen, A. Elberg, and J. Larmarange. 2018. GGally: extension to "ggplot2." https://CRAN.R-project.org/package=GGally

Schwartz, A. M., A. F. Hinckley, P. S. Mead, S. A. Hook, and K. J. Kugeler. 2017. Surveillance for Lyme disease — United States, 2008–2015. MMWR Surveill. Summ. 66: 1–12.

Spielman, A., C. M. Clifford, J. Piesman, and M. D. Corwin. 1979. Human Babesiosis on Nantucket Island, USA: description of the vector, Ixodes (Ixodes) Dammini, N. Sp. (Acarina: Ixodidae)1. J. Med. Entomol. 15: 218–234.

Spielman, A., J. Piesman, P. Etkind, T. K. Ruebush, D. D. Juranek, and M. S. Jacobs. 1981. Reservoir hosts of human babesiosis on Nantucket Island. Am. J. Trop. Med. Hyg. 30: 560–565.

Spielman, A., M. L. Wilson, J. F. Levine, and J. Piesman. 1985. Ecology of Ixodes dammini-borne human babesiosis and Lyme disease. Annu. Rev. Entomol. 30: 439–460.

Stafford, K. C., S. C. Williams, L. A. Magnarelli, A. Bharadwaj, S.-H. Ertel, and R. S. Nelson. 2014. Expansion of zoonotic babesiosis and reported human cases, Connecticut, 2001–2010. J. Med. Entomol. 51: 245–252.

Stephenson, N., and J. Foley. 2016. Parallelisms and contrasts in the diverse ecologies of the Anaplasma phagocytophilum and Borrelia burgdorferi complexes of bacteria in the far Western United States. Vet. Sci. 3: 26.

Telford, S. R., 3rd, J. E. Dawson, P. Katavolos, C. K. Warner, C. P. Kolbert, and D. H. Persing. 1996. Perpetuation of the agent of human granulocytic ehrlichiosis in a deer tick-rodent cycle. Proc. Natl. Acad. Sci. U. S. A. 93: 6209–6214.

Telford, S. R., 3rd, and A. Spielman. 1993. Reservoir competence of white-footed mice for Babesia microti. J. Med. Entomol. 30: 223–227.

Tennekes, M. 2018. tmap : Thematic Maps in R. J. Stat. Softw. 84.

Thapa, S., Y. Zhang, and M. S. Allen. 2019. Effects of temperature on bacterial microbiome composition in Ixodes scapularis ticks. MicrobiologyOpen. 8: e00719.

Tran, P. M., and L. Waller. 2013. Effects of landscape fragmentation and climate on Lyme disease incidence in the northeastern United States. Ecohealth. 10: 394–404.

Tran, T., M. A. Prusinski, J. L. White, R. C. Falco, V. Vinci, W. K. Gall, K. Tober, J. Oliver, L. A. Sporn, L. Meehan, et al. 2020. Spatio-temporal variation in environmental features predicts the distribution and abundance of Ixodes scapularis. Int. J. Parasitol. S0020751920303313.

United States Census Bureau. 2000. Appendix A: Census 2000 Geographic Terms and Concepts. https://www2.census.gov/geo/pdfs/reference/glossry2.pdf

United States Census Bureau. 2013. American Community Survey, 2013 5-year estimates. https://www.census.gov/data/tables.html

United States Census Bureau. 2019. TIGER/line shapefile, 2019, 2010 Nation, U.S., 2010 census 5-Digit ZIP Code Tabulation Area (ZCTA5) National. (https://catalog.data.gov/dataset/tiger-line-shapefile-2019-2010-nation-u-s-2010-census-5-digit-zip-code-tabulation-area-zcta5-na).

Vail, S. G., and G. Smith. 1998. Air temperature and relative humidity effects on behavioral activity of blacklegged tick (Acari: Ixodidae) nymphs in New Jersey. J. Med. Entomol. 35: 1025–1028.

Werden, L., L. R. Lindsay, I. K. Barker, J. Bowman, E. K. Gonzales, and C. M. Jardine. 2015. Prevalence of Anaplasma phagocytophilum and Babesia microti in Ixodes scapularis from a newly established Lyme disease endemic area, the Thousand Islands Region of Ontario, Canada. Vector Borne Zoonotic Dis. 15: 627–629.

White, D. J., J. Talarico, H. G. Chang, G. S. Birkhead, T. Heimberger, and D. L. Morse. 1998. Human babesiosis in New York State: review of 139 hospitalized cases and analysis of prognostic factors. Arch. Intern. Med. 158: 2149–2154.

Wickham, H. 2016. ggplot2: elegant graphics for data analysis, 2nd ed. 2016. ed, Use R! Springer International Publishing : Imprint. Springer, Cham, Switzerland.

Xu, L., A. D. Paterson, W. Turpin, and W. Xu. 2015. Assessment and selection of competing models for zero-inflated microbiome data. PLoS One. 10: e0129606.

Yang, L., S. Jin, P. Danielson, C. Homer, L. Gass, S. M. Bender, A. Case, C. Costello, J. Dewitz, J. Fry, et al. 2018. A new generation of the United States National Land Cover Database: requirements, research priorities, design, and implementation strategies. ISPRS J. Photogramm. Remote Sens. 146: 108–123.

Zeileis, A., C. Kleiber, and S. Jackman. 2008. Regression models for count data in R. J. Stat. Softw. 27: 1–25.

Zhen, Z., L. Shao, and L. Zhang. 2018. Spatial hurdle models for predicting the number of children with lead poisoning. Int. J. Environ. Res. Public. Health. 15: 1792.